ACS APPLIED MATERIALS & INTERFACES

Research Article

www.acsami.org

# Li-Ion Adsorption and Diffusion on Two-Dimensional Silicon with Defects: A First Principles Study

Jeffry Setiadi,[†] Matthew D. Arnold,[†] and Michael J. Ford*,[†]

School of Physics and Advanced Materials, University of Technology, Sydney, P.O. Box 123, Broadway, New South Wales 2007, Australia

**ABSTRACT:** Using first principles calculations we investigate the binding and diffusion of Li on silicene and evaluate the prospects for application to Li-ion batteries. We find that the defect formation energy for silicene is half that of graphene, showing that silicene is more likely to contain defects. The overall lithium adsorption energy on silicene with defects is greater than the bulk cohesive energy of lithium giving stability for use in storage. Our results predict high mobility for lithium atoms on the surface of silicene with energy barriers in the range of 0.28−0.30 eV. Further, we find that the diffusion barrier through silicene is significantly lower than the diffusion barrier through graphene, with a value of 0.05 eV for the double vacancy and 0.88 eV for the single vacancy. The low diffusion barriers, both on the surface and through the hollow site, suggest a suitable material for use in Li-ion batteries.

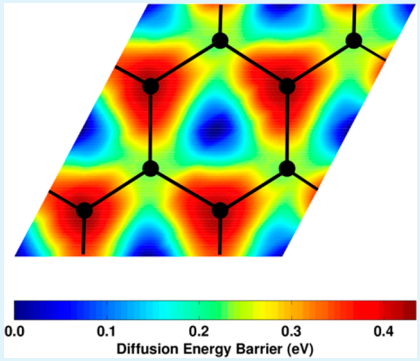


**KEYWORDS:** *silicene, lithium, first-principles calculations, diffusion of lithium, defects in silicene*

## 1. INTRODUCTION

As the demand for portable energy sources increases, improvements in Li-ion batteries (LIBs) have become an important quest. The conventional material used as the anode is graphite, which has a theoretical maximum specific capacity of 372 mA h/g. However, this capacity cannot meet the standards of current and future technology.

An alternative to graphite is its two-dimensional (2D) form called graphene, which is simply a single layer of graphite. Since its first isolation in 2004,[1,2] potential applications of graphene have been considered. Computational studies have shown the theoretical capacity for graphene is higher than that of its bulk form graphite. However, an experimental study has shown that the capacity of a single layer of graphene is less than a few layers of graphene.[3] Single layer graphene allows binding of Li atoms on opposite sides of the sheet, increasing Coulomb repulsion and hence decreasing the Li binding energy compared to multiple layers of graphene. In addition the bulk cohesive energy of Li is 1.80 eV,[4] which causes Li atoms to cluster and not disperse on the graphene surface giving rise to small surface coverage.

Recently a 2D silicon (Si) material called silicene, analogous to graphene, was grown on an Ag (110) surface.[5] Theoretical studies have shown similar characteristics between graphene and silicene, but one distinct feature is the buckling of Si atoms.[6] The possible use in LIBs has also been investigated.[7] In this study it was shown that the Li adsorption energy on silicene is much higher than that of graphene. In addition the surface diffusion energy barrier is relatively low at 0.22 eV. Hence, silicene may be an alternative to graphene as an anode material. A review article by Kara et al. contains more detailed information about the growth mechanisms and theoretical investigations of silicene.[8]

In this paper we present further computational investigation of the interaction of Li with silicene. In particular we investigate defects in silicene, and the interaction of Li on these defects. In addition to adsorption energies we also investigate surface diffusion and diffusion through silicene to get insights on its cyclic performance. We evaluate our silicene findings against comparable results that have been reported for graphene.

## 2. METHOD

The interaction of Li with silicene was investigated using density functional theory (DFT) as part of the SIESTA software package.[9] We chose the generalized-gradient approximation (GGA) for the exchange-correlation functional as parameterized by Perdew, Burke, and Ernzerhof (PBE).[10] Electrons are described with norm-conserving Troullier−Martins[11] pseudopotentials with a double-zeta polarization (DZP) basis set. These pseudopotentials are taken from the SIESTA database and were originally developed for use with the ABINIT DFT code.[12] Use of a double-zeta plus polarization basis set is relatively standard and represents a good compromise between efficiency of the calculation and representation of the electronic states. In SIESTA the pseudized atomic orbitals are strictly confined within a specified cut-off radius determined from the energy shift parameter representing the increase in energy of an orbital because of this confinement. Hence, energy shift is an important parameter for determining the convergence of a calculation, the default value of 20 mRy is quite poor. In the present calculations an energy shift of 5 mRy was used throughout, and total energies are converged to better than 0.1 eV at this value. A mesh cut-off of 450 Ry was used, giving a total energy

**Received:** July 15, 2013
**Accepted:** October 3, 2013
**Published:** October 3, 2013

  

convergence of about 0.002 eV. The mesh cut-off parameter represents the highest energy plane-wave that can be represented on the integration grid.

SIESTA always imposes periodic boundary conditions, so our surfaces are represented by repeating slabs. To avoid slabs interacting with their periodic images we use a vacuum gap in the unit cell of 10 Å: this is sufficient because the largest orbital radius defined by the energy shift above is approximately 5 Å. Structural relaxations were performed using the Broyden[13] method with a force tolerance of 0.04 eV/Å and the Brillouin zone was sampled with an 8 × 8 × 1 Monkhorst–Pack grid.[14] Force tolerances up to 0.01 eV/A have been tested and give essentially identical results. A k-point grid of 20 × 20 × 1 changes the total energy by only 0.002 eV.

We studied defects on silicene by calculating the defect formation energies using eq 1 below with a 6 × 6 supercell of the primitive unit cell. A supercell of this size is sufficient to prevent defects from interacting with their periodic images in the plane of the slab.

$$E_f = E_{defect} - \frac{N-i}{N}E_{Pristine} \quad (1)$$

$E_{defect}$ and $E_{pristine}$ are the total energy of the defective and the non-defective structures respectively, $N$ is the number of atoms in the pristine unit cell, and $i$ is the number of atoms removed. Li adsorption and diffusion were studied using a slightly smaller 4 × 4 supercell to maintain a reasonable computational time without compromising reliability. Based on our calculations of lithium adsorption on 4 × 4 and 6 × 6 graphene supercells, we found the energy to differ by only 0.02 eV. The adsorption energy was calculated using eq 2 below.

$$E_{ad} = \frac{1}{N}(NE_{Li} + E_{Si} - E_{NLi+Si}) \quad (2)$$

In eq 2, $N$ represents the number of Li atoms in the system, $E_{Li}$ is the energy of a single Li atom, $E_{Si}$ is bare silicene and $E_{Li+Si}$ is the total energy of the system containing both Li and silicene. Basis set superposition error (BSSE) correction was used for calculating $E_{Li}$ and $E_{Si}$ with the counterpoise method.[15] In addition, spin polarization was included to calculate $E_{Li}$ and structures with an odd number of electrons.

## 3. RESULTS

**3.1. Defects in Silicene.** The defects we are interested in are those that have been studied previously for graphene,[16,17] the single vacancy (SV) and double vacancy (DV) and the Stone–Thrower–Wales (STW) defect.[18] Vacancies in bulk silicon structures have already been investigated both theoretically and experimentally with the exception of the STW defect.[19,20] The equilibrium structures for the various defects and for pristine silicene are shown in Figure 1.

To validate our calculations we compare the pristine structure to already established results in the literature for the Si–Si bond, lattice constant $a$, and buckling height $\Delta z$. Our values for these are 2.31 Å, 3.90 Å, and 0.50 Å, respectively. Osborn and co-workers[21] also used an atomic orbital DFT method and found a bond length of 2.30 Å, which is a very similar value to ours. Next, Cahangirov et al.[7,22] and Huang et al.[7] reported lattice constants of 3.90 Å and 3.86 Å respectively. Finally, various authors reported slightly different values for the buckling height in the range of 0.44–0.55 Å.[21−23] Our value of buckling height lies within those calculated using atomic orbitals while the smaller buckling heights reported were obtained with plane wave calculations. Our structural parameters are in good agreement with those of the literature.

We further investigate the nature of these defects in silicene by calculating the defect formation energy $E_f$ using eq 1, the results are given in Table 1. Formation energies for the SV and DV defects are approximately the same for silicene and for bulk Si. The formation energy for the STW defect is less than the two previous vacancies because it does not require removal of atoms, but only reorientation of the bonds. Hence, there is a lower penalty from bond breaking.

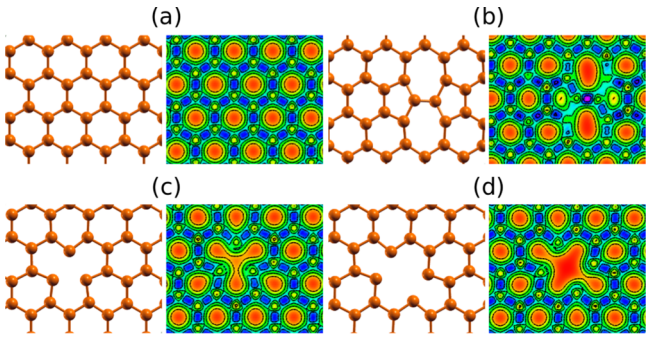


**Figure 1.** Structures of silicene and its corresponding charge density plot of (a) pristine, (b) STW, (c) SV, and (d) DV. Scale starts at 0 (red) and increases to 0.1 (purple).

**Table 1. Defect Formation Energies $E_f$ of Defects on Silicene and Graphene**

| $E_f$ (eV) | SV | DV | STW |
|---|---|---|---|
| silicene | 3.60 | 4.45 | 2.57 |
| bulk silicon | 4.00[a] | 4.63[b] | |
| graphene | 7.70 (7.40)[c] | 7.45 (7.00)[c] | 6.13 (6.02)[d] |

[a]Ref 19. [b]Ref 31. [c]Ref 16. [d]Ref 24.

We have also calculated the corresponding formation energies in graphene for comparison (Table 1) as this is a well-studied system. Our results are in reasonable agreement with previous calculated values for the three defects in carbon structures. The vacancies were studied on graphite with a first principles method while the STW defect was studied in graphene using a semi-empirical method.[16,24]

Formation energies in graphene are double that of silicene because of the weaker bond between silicon atoms (220 kJ) compared with carbon atoms (350 kJ). The larger silicon atom increases the interatomic distance between Si atoms, and hence decreases $\pi$–$\pi$ overlap, leading to weaker bonding compared with carbon.[25] For the application to LIBs, our results on defected silicene suggest that investigating the interaction of lithium on silicene with defects is crucial as defects are more likely to be present in silicene than in graphene.

**3.2. Lithium Adsorption.** Previously reported calculations show that the hollow site is the most stable site for lithium adsorption.[7,26] We also tested this by placing the Li on top of the bridge site (B), buckled silicon atom (Si-$\alpha$), silicon atom in the bottom plane (Si-$\beta$), and the hollow site (H) and then relaxing the full structure except restraining the lateral position of the Li atom on the surface. We found that the hollow site is the most stable by at least 1.00 eV (compared to the top and bridge sites).

We calculated the lithium adsorption energy using eq 2 for the pristine case and obtained a value of 1.89 eV with a Li–Si bond length of 2.78 Å and perpendicular distance of 1.59 Å. Our value of perpendicular distance is in good agreement with Huang et al.;[7] however, the adsorption energy is smaller than those of the studies of Osborne et al.[26] and Huang et al.[7] who found values of 2.21 eV and 2.45 eV,[7] respectively. A recalculation with the SIESTA van der Waals (VDW)

Table 2. Perpendicular Height $\Delta z_{Li}$, Bond Length $r$, and Lithium Adsorption Energy $E_{ad}$ for Both Silicene and Graphene

| | | H | SV | DV | STW |
|---|---|---|---|---|---|
| Si | $\Delta z_{Li}$ (Å) | 1.59 (1.53)[a] | 1.37 | 0.10, 0.36 | 1.47 |
| | $r$ (Å) | 2.78 | 2.31 | 3.53 | 2.73 |
| | $E_{ad}$ (eV) | 1.89 (2.21)[b] | 2.69, 3.85 | 3.15 | 1.99 |
| C | $\Delta z_{Li}$ (Å) | 1.80 (1.84)[c] | 1.75 | 1.50 | 1.70 |
| | $r$ (Å) | 2.31 (2.35)[d] | 2.21 (2.03)[d] | 2.32 (2.23)[d] | 2.25 (2.22)[d] |
| | $E_{ad}$ (eV) | 0.99 (1.01)[e] | 2.71 (3.12)[d] | 2.07 (2.23)[f] | 1.62 (1.94)[d] |

[a]Ref 7. [b]Ref 26. [c]Ref 32. [d]Ref 30. [e]Ref 33. [f]ref 29.

exchange-correlation functional parameterized by Dion et al.[27] for lithium on pristine silicene gave an adsorption energy 0.10 eV smaller. Hence, long range interaction with silicene is small and can be ignored.

The calculation of Huang et al.[7] is based on a plane-wave DFT calculation using the PW91 exchange-correlation functional; hence we might expect a difference to our result. The result of Osborn and co-workers,[26] however, is a SIESTA calculation using the same GGA functional. The large difference observed here is most likely due to the different computational conditions used. It is unclear what orbital confinement is used and whether their adsorption energies are BSSE corrected. Using the default energy shift parameter and no BSSE corrections with a 2 × 2 supercell we obtain an adsorption energy of 2.21 eV, a value close to that of Osborn and co-workers.[26] We have also calculated the average adsorption energies of 2, 4, and 8 lithium adatoms and find values of 2.05 eV, 2.50 eV, and 2.23 eV, respectively. This trend of increasing adsorption energy with increasing lithium coverage follows the results of both of these authors.

To further investigate the reliability of our calculations we have calculated adsorption of a single lithium atom on pristine and defective graphene, as this is a well-studied system. The results are given in Table 2 along with previous calculations. In addition the relaxed structures are shown in Figure 2. Comparison of the absolute magnitude of our results with previous calculations is difficult given the variety of methods employed; however the trends in these data are consistent.

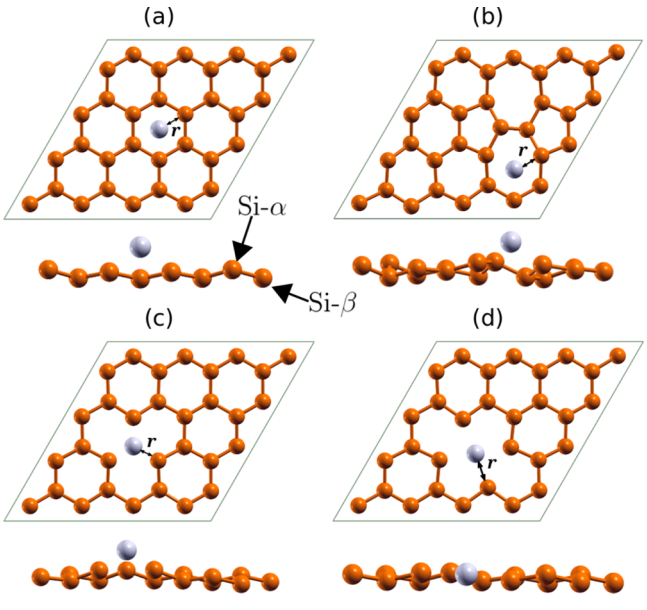


Figure 2. Top and side view of lithium adsorbed on (a) pristine, (b) STW, (c) SV, and (d) DV silicene.

Our results for adsorption of lithium on pristine silicene and the three defects are also given in Table 2. The adsorption sites for the defects are chosen based on the charge density plot in Figure 1. The center of the DV defect and the heptagon of the STW defect are the adsorption sites respectively. For the SV defect two sites are considered, the center of the vacancy and the hexagon hollow sites surrounding the vacancy. This is primarily because the charge density plots hint that the three hollow sites surrounding the vacancy are more stable.

The bond lengths for adsorption onto graphene are all shorter than the corresponding values for silicene. This is due to the longer bond length between silicon atoms creating much larger hollow sites. Another parameter we note is the perpendicular distance between lithium and silicene. For the SV and STW defects we calculated values of 1.37 Å and 1.47 Å, respectively. However, the peculiar value is that of the DV defect having a perpendicular distance of 0.10 Å below the buckled silicon atom (Si-$\alpha$) and 0.36 Å above the bottom silicon atom (Si-$\beta$). To see the effect of this we calculated the adsorption energy for the defects. The energy for the DV defect is large compared to the other structures except for the hexagon site of the SV defect. The size of the adsorption energy and the perpendicular distance suggest that the lithium atom is trapped inside the vacancy.

Finally, we compare the adsorption energies to the corresponding graphene structures. Osborne et al.[26] and Huang et al.[7] have already shown that lithium on pristine silicene gives larger adsorption energy than lithium on pristine graphene. We calculate the same result for the pristine case and in addition we find that the adsorption energies are much larger than the bulk lithium cohesive energy. It is also possible for graphene to achieve the same behavior through its defects. However, silicene has the advantage that the pristine form is able to disperse lithium atoms on its surface while graphene requires some form of defect to achieve the same result.

**3.3. Surface Diffusion.** Surface diffusion is important because it determines cyclic performance of LIBs. Huang et al.[7] and Tritsaris et al.[28] calculated the energy barrier for lithium on pristine silicene as 0.22 eV and 0.23 eV, respectively, using the nudged elastic band (NEB) method. Here we report the energy barriers for diffusion of lithium on the surface of silicene with and without defects. These values were calculated by mapping out the entire potential energy surface for Li on silicene. The Li atom is scanned across the surface and geometry optimizations performed at each point in this scan. All the silicon atoms and the perpendicular coordinate of the Lithium atom are relaxed at each point while the lateral position of the Li is constrained. A grid of 11 × 11 points was calculated for each case, and a mesh interpolation was used to generate the contour plots in Figure 3. The energies are normalized with respect to the smallest

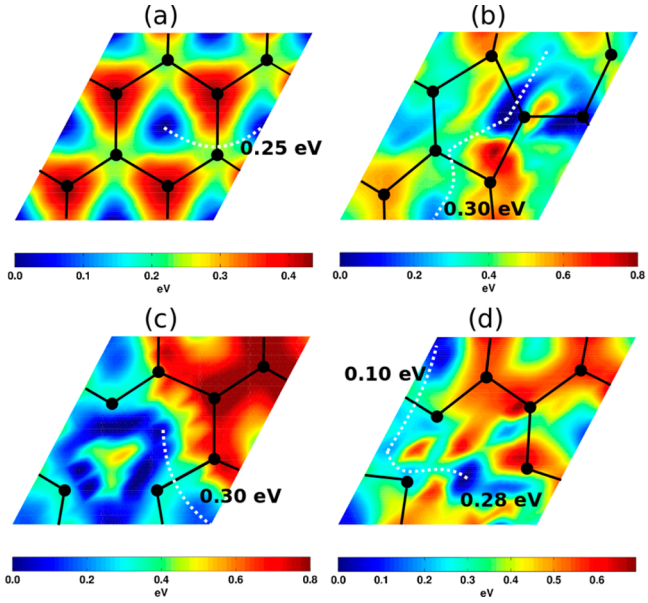


**Figure 3.** Pseudo-color plot of energy diffusion barriers of lithium on the surface of (a) pristine, (b) STW, (c) SV, and (d) DV silicene. The initial positions of Silicon atoms, in the absence of Lithium on the surface, are drawn. The minimum energy paths to transition out to a pristine hollow site are shown with a dashed line.

energy on the contour. In addition silicon atoms are drawn on Figure 3 to show their initial positions in the absence of the lithium interaction. The silicon atoms will move as the Lithium atom is moved around on the surface. Our method for determining the minimum energy diffusion paths (MEP), while more time consuming, gives the same result as the nudged elastic band (NEB) method. Rather than efficiently finding only the MEP, as is the case with NEB, we map out the full potential energy surface. The contour plots in Figure 3 are generated using an interpolation scheme purely for cosmetic reasons; the raw data grid is sufficiently fine to determine the potential energy surface quite unambiguously: it is unlikely we have missed any details in the potential energy surface with this 11 × 11 grid of points.

Starting with pristine silicene in Figure 3 the minimum energy path is not a straight line between two hollow sites. By looking at the barrier height the path between two hollow sites is a curve bent towards a silicon atom. The corresponding energy barrier is about 0.25 eV. Huang et al.[7] and Tritsaris et al.[28] also reported a similar path and barrier height. This barrier height is small and suggests high mobility for lithium atoms on the surface. Even with the extreme case where lithium diffuses across a buckled silicon atom the energy barrier is less than 0.45 eV from our plot. As suggested by Huang et al.,[7] pristine silicene is a candidate for applications in LIBs because of this behavior.

This low energy barrier is also observed with defects. For lithium to diffuse out of the STW defect heptagon ring to a pristine hollow site would require a two-step transition. First it would diffuse out of the small pentagon ring and then transition to a pristine hollow site with a barrier of 0.30 eV. For the SV defect we noticed that there is a local minimum around the center of the defect, and the only way out is to transition from the small hexagon. The barrier for this is around 0.30 eV. Diffusion out of the center of the DV defect is also a two-step transition with the first to one of its smaller pentagons and then to a pristine site. Also much like the pristine case the highest barrier is less than 1.00 eV meaning that the potential energy surface of silicene is relatively flat and will allow lithium atoms to diffuse across its surface with ease. We compare this to results by Fan et al. who showed that the energy barriers for Li diffusion on graphene with vacancies are in the range of 0.17−0.56 eV.[29] Hence, lithium diffusion on silicene is similar to graphene with respect to energy barriers.

An interesting observation from Figure 3 is that lithium can easily move away from the center of the DV defect and the small hexagon of the SV defect. We mentioned earlier that the Li adsorption energy on the DV and SV defects is quite high but as evident with the low energy barriers lithium can move out of the site easily. Therefore, the high adsorption energy for both the DV and the SV defects will not hinder the cycle performance of silicene because thermal energy can move lithium atoms away during intercalation.

**3.4. Diffusion through Silicene.** Another important aspect of the interaction of lithium with silicene is diffusion through the hollow sites. It is important to investigate this because 2D materials would likely be stacked in layers as the surface-to-volume ratio is higher than having only a single sheet. Yao et al.[30] and Fan et al.[29] investigated lithium diffusion through the hollow sites of graphene and found high energy barriers. This means that lithium atoms will have a low probability of diffusing through graphene. To compare silicene with graphene we also investigated the diffusion barriers through silicene; the results are summarized in Table 3.

**Table 3. Li Energy Barriers through the Hollow Sites of Silicene and Graphene**

| | H | SV | DV | STW |
|---|---|---|---|---|
| Si | 1.59 | 3.10, 0.88 | 0.05 | 0.86 |
| C | 8.38 (9.80)[a] | 5.30 (6.22)[a] | 1.72 (1.55)[a] | 4.98 (6.35)[b] |

[a]Ref 29. [b]Ref 30.

Diffusion barriers through the silicene sheet were determined by mapping out the potential energy surface in a manner similar to surface diffusion above. The lithium atom was fixed at sequential heights above the surface, and geometry optimizations were performed keeping the Li height constrained. The Li atom can relax perpendicular to the diffusion path allowing us to identify the minimum energy path without the need to scan in two directions.

Comparing our results for graphene with previous values we see the same trend between the pristine and defective surfaces. The value for pristine graphene suggests that it is nearly impossible for lithium to diffuse through it. In contrast, our value for pristine silicene suggests the opposite and thus lithium atoms can diffuse through the hollow site with a high probability. The smaller energy barrier can be explained by comparing the structures of silicene and graphene. The lattice constant for silicene is 3.90 Å while for graphene it is 2.46 Å. This means that the area of the hollow site is smaller than that of silicene. The larger area for silicene makes it easier for lithium to diffuse through.

The energy barriers for defects also show the same behavior with significantly lower energy barriers compared to graphene. For the two sites of the SV defect we found very different energy barriers. Diffusing through the center requires 3.10 eV but through the hexagon site only 0.88 eV is needed. This can be explained by the charge density plot in Figure 1 where there

is more charge surrounding the center because of dangling bonds. Hence, lithium would choose to diffuse through the hexagon site as its minimum energy path. For the DV and the STW defects the path is through the large octagon and heptagon respectively at 0.05 eV and 0.86 eV. The energy barriers for all are significantly lower than its graphene counterpart and hence we predict silicene to be a very porous material that can allow lithium atoms to diffuse through its hollow sites.

## 4. CONCLUSION

We have undertaken DFT calculations of the defect formation energies in silicene, the binding of Li atoms to these defects, and its diffusion across and through silicene. Our motivation is to evaluate the use of this novel material in lithium ion batteries and to compare its potential performance to graphene. We have focused our investigation on the single and double-vacancy defects as well as the Stone−Thrower−Wales defect as these have been the most commonly investigated in previous reports.

The three defects studied are predicted to have lower formation energies in silicene than the corresponding defects in graphene. In graphene they all have formations energies greater than 6 eV, whereas in silicene they range between approximately 2.5 eV to 3.5 eV. This indicates that defects are more likely to form in silicene than in graphene, and this could be beneficial in lithium ion battery applications as defects play a crucial role in binding Li atoms. In all cases, Li is more strongly bound to silicene compared with graphene: 1.89−3.85 eV compared with 0.99−2.71 eV. Furthermore, in silicene the adsorption energies are all higher than the Li bulk cohesive energy. From this we expect Li to disperse on the surface of a single silicene layer better than graphene and hence improve battery capacity.

Diffusion of lithium atoms across and through the substrate is also an important consideration in the cycle performance of a battery. The overall diffusion across the silicene surface is similar to the diffusion across the surface of graphene. However, the main difference between the two materials is that Li diffusion through hollow sites is mediated by a significantly lower energy barrier than graphene: 1.59 eV versus 8.38 eV for the pristine case, and 0.05 eV versus 1.72 eV for the double-vacancy. Interestingly, although the diffusion barrier through pristine graphene is higher than the three defects studied, in silicene the barrier through the center of the single-vacancy is the highest. This is presumably due to the dangling bonds present. However, in this case Lithium atoms would choose its neighboring smaller hexagon site to diffuse through as only 0.88 eV is required. Overall, silicene is a relatively porous material resulting in high Li mobility. Therefore, based on first principles calculations we predict that silicene may be superior to graphene for LIBs because of low energy barriers and higher adsorption energies.

## AUTHOR INFORMATION


### Corresponding Author

*E-mail: mike.ford@uts.edu.au. Phone: +61 2 9514 7956. Fax: +61 2 9514 2219.

### Author Contributions

†These authors contributed equally.


### Author Contributions

The manuscript was written through contributions of all authors. All authors have given approval to the final version of the manuscript.

### Notes

The authors declare no competing financial interest.

## ACKNOWLEDGMENTS

This research was supported by the National Computational Infrastructure (NCI) through their merit allocation scheme and used NCI resources iVEC@Murdoch and facilities in Canberra, Australia.

## REFERENCES


(1) Geim, A. K. *Science* **2009**, *324*, 1530−1534.
(2) Novoselov, K. S.; Geim, A. K.; Morozov, S. V.; Jiang, D.; Zhang, Y.; Dubonos, S. V.; Grigorieva, I. V.; Firsov, A. A. *Science* **2004**, *306*, 666−669.
(3) Pollak, E.; Geng, B.; Jeon, K.-J.; Lucas, I. T.; Richardson, T. J.; Wang, F.; Kostecki, R. *Nano Lett.* **2010**, *10*, 3386−3388.
(4) Doll, K.; Harrison, N. M.; Saunders, V. R. *J. Phys.: Condens. Matter* **1999**, *11*, 5007.
(5) Aufray, B., K. A.; Vizzini, S.; Oughaddou, H.; LeEandri, C.; Ealet, B.; Le Lay, G. *Appl. Phys. Lett.* **2010**, *96*, 183102.
(6) Takeda, K.; Shiraishi, K. *Phys. Rev. B* **1994**, *50*, 14916−14922.
(7) Huang, J.; Chen, H.-J.; Wu, M.-S.; Liu, G.; Ouyang, C.-Y.; Xu, B. *Chin. Phys. Lett.* **2013**, *30*, 017103.
(8) Kara, A.; Enriquez, H.; Seitsonen, A. P.; Voon, L.; Vizzini, S.; Aufray, B.; Oughaddou, H. *Surf. Sci. Rep.* **2012**, *67*, 1−18.
(9) Soler, M., A. E.; Gale, J. D.; Garcia, A.; Junquera, J.; Ordejon, P.; Sanchez-Portal, D. *J. Phys.: Condens. Matter* **2002**, *14*, 2745.
(10) Perdew, J. P.; Burke, K.; Ernzerhof, M. *Phys. Rev. Lett.* **1996**, *77*, 3865−3868.
(11) Troullier, N.; Martins, J. L. *Phys. Rev. B* **1991**, *43*, 1993−2006.
(12) *SIESTA*; http://icmab.cat/leem/siesta/ (accessed August 10, 2012).
(13) Shanno, D. F. *Math. Comput.* **1971**, *24*, 647−656.
(14) Monkhorst, H. J.; Pack, J. D. *Phys. Rev. B* **1976**, *13*, 5188−5192.
(15) Boys, S. F.; Bernardi, F. *Mol. Phys.* **1970**, *19*, 553−566.
(16) El-Barbary, A. A.; Telling, R. H.; Ewels, C. P.; Heggie, M. I.; Briddon, P. R. *Phys. Rev. B* **2003**, *68*, 144107.
(17) Krasheninnikov, A. V.; Lehtinen, P. O.; Foster, A. S.; Nieminen, R. M. *Chem. Phys. Lett.* **2006**, *418*, 132−136.
(18) Stone, A. J.; Wales, D. J. *Chem. Phys. Lett.* **1986**, *128*, 501−503.
(19) Fukata, N.; Kasuya, A.; Suezawa, M. *Phys. B* **2001**, *308*, 1125−1128.
(20) Seong, H.; Lewis, L. J. *Phys. Rev. B* **1996**, *53*, 9791−9796.
(21) Osborn, T. H.; Farajian, A. A.; Pupysheva, O. V.; Aga, R. S.; Lew Yan Voon, L. C. *Chem. Phys. Lett.* **2011**, *511*, 101−105.
(22) Cahangirov, S.; Topsakal, M.; Akturk, E.; Sahin, H.; Ciraci, S. *Phys. Rev. Lett.* **2009**, *102*, 236804.
(23) Ding, Y.; Ni, J. *Appl. Phys. Lett.* **2009**, *95*, 083115−083115-3.
(24) Zhou, L. G.; Shi, S. Q. *Appl. Phys. Lett.* **2003**, *83*, 1222−1224.
(25) Zhang, R. Q.; Lee, S. T.; Law, C. K.; Li, W. K.; Teo, B. K. *Chem. Phys. Lett.* **2002**, *364*, 251−258.
(26) Osborn, T. H.; Farajian, A. A. *J. Phys. Chem. C* **2012**, *116*, 22916−22920.
(27) Román-Pérez, G.; Soler, J. M. *Phys. Rev. Lett.* **2009**, *103*, 096102.
(28) Tritsaris, G. A.; Kaxiras, E.; Meng, S.; Wang, E. G. *Nano Lett.* **2013**, *13*, 2258−2263.
(29) Fan, X.; Zheng, W. T.; Kuo, J.-L. *ACS Appl. Mater. Interfaces* **2012**, *4*, 2432−2438.
(30) Yao, F.; Guenes, F.; Ta, H. Q.; Lee, S. M.; Chae, S. J.; Sheem, K. Y.; Cojocaru, C. S.; Xie, S. S.; Lee, Y. H. *J. Am. Chem. Soc.* **2012**, *134*, 8646−8654.
(31) Banhart, F.; Kotakoski, J.; Krasheninnikov, A. V. *ACS Nano* **2011**, *5*, 26−41.

(32) Zheng, J.; Ren, Z.; Guo, P.; Fang, L.; Fan, J. *Appl. Surf. Sci.* **2011**, *258*, 1651−1655.
(33) Valencia, F.; Romero, A. H.; Ancilotto, F.; Silvestrelli, P. L. *J. Phys. Chem. B* **2006**, *110*, 14832−14841.